ISSN 1024-8560, Atmospheric and Oceanic Optics, 2018, Vol. 31, No. 3, pp. 269–272. © Pleiades Publishing, Ltd., 2018.
Original Russian Text © A.I. Grishin, A.V. Kryuchkov, 2018, published in Optika Atmosfery i Okeana.

REMOTE SENSING OF ATMOSPHERE, HYDROSPHERE, AND UNDERLYING SURFACE

Lidar Observations of Atmospheric Optical Characteristics during Sichuan Earthquake

A. I. Grishin[a, *] and A. V. Kryuchkov[a, b, **]

[a] *V.E. Zuev Institute of Atmospheric Optics, Siberian Branch, Russian Academy of Sciences, Tomsk, 634055 Russia*
[b] *Tomsk State University, Tomsk, 634050 Russia*
**e-mail: aig@iao.ru*
***e-mail: kaw@iao.ru*

Received January 29, 2017

Abstract—The results of lidar observations of the atmosphere during the Sichuan (China) earthquake of 2008 are presented. It is shown that atmospheric parameters substantially changed during and after the earthquake. The profile of scattering characteristics formed in the lower troposphere differs from the original, which can serve as a predictor for earthquakes.

Keywords: earthquake, atmosphere, lidar, aerosol concentration, boundary layer
DOI: 10.1134/S1024856018030053

INTRODUCTION

Earthquakes belong to the group of the most destructive natural cataclysms. Strong earthquakes with the magnitude $M > 7$ are commonly accompanied by multiple human victims and considerable destruction even at significant distances from the epicenter. It is sufficient to remember the California earthquake (1906), Ashkhabad (1948), Spitak (1988), Iran (1990), Indonesia (2006), and so on. This series can be supplemented by the Sichuan earthquake (China) of 2008. According to different sources, from 70 to 90 thousand lives were lost during that earthquake. Every year, more than 100 dangerous and potentially hazardous earthquakes occur on the Earth.

Therefore, the prognosis of the place and time of destructive shocks remains an important problem. At the present time, such predictors of earthquakes as strengthening fluctuations of geophysical fields of different natures (acoustic, electric, biological, etc.) are known, as well as atmospheric phenomena, including those which proceed in the upper atmospheric layers. Data from observations at these altitudes during earthquake events are extensive [1–5], including satellite data [4, 5, 7]. Investigations of transformation of tropospheric optical characteristics during different natural cataclysms, particularly in the lower troposphere, are much more modest [6, 8].

This work describes fluctuations of atmospheric optical characteristics during the Sichuan earthquake of 2008. The aim of the work is to show that sharp variations in optical characteristics of the atmosphere under stable atmospheric conditions and in the absence of fronts can serve as a predictor of a future earthquake, along with other geophysical signs.

MEASUREMENT CONDITIONS AND INSTRUMENTATION

In 2008, one of the authors of this work was on a business trip in Loyan (China), where a laser locator, working at the Institute of Atmospheric Optics, Siberian Branch, Russian Academy of Sciences, and produced in China, was tested. During the Sichuan earthquake, which started on May 12, 2008, at 14:28 Beijing time, the lidar was located on the experimental site and was switched on. Precisely that circumstance allowed us to obtain the experimental data which became the basis of this work.

The optical and operational parameters of the lidar are given below.

Laser radiation wavelength	915 nm
Emitter type	Semiconductor laser diode
Optical receiver	Lens
and emitting system types	Aspherical
Emitting aperture diameter	110 mm
Pulse length	100 ns
Pulse power	2.5 μW
Pulse repetition rate	20 kHz
Photoreceiver type	Avalanche photodiode
Receiving aperture diameter	110 mm

Half-width of interferential filter	100 nm
Time of signal accumulation (set by operators)	1 s to 10 min
Maximal sounding altitude	7.5 km

The town of Loyan is situated 900 km northeast from Sichuan. Nonetheless, shocks of 3–4 magnitude were distinctly felt there. The cataclysm was accompanied by such signs as rocking chandeliers, ringing dishes, anomalous behavior of animals immediately before underground shocks, broken window glass, and more. The earthquake was also recorded in the neighboring countries of India, Pakistan, Thailand, Vietnam, Mongolia, and Russia.

Backscattered signals received by the lidar were averaged over 5 minutes (6 million instances) and recorded on the hard disk, then processed, during which the altitude profiles of the scattering coefficient $\alpha(R)$ were retrieved at the sounding distance R.

Profiles of $\alpha(R)$ were retrieved by the Klett method [9]:

$$\alpha(R) = \frac{S(R)}{\frac{S(R_{\max})}{\alpha(R_{\max})} + 2\int_{R}^{R_{\max}} S(R)dR}. \quad (1)$$

Here $S(R) = \frac{U(R)R^2}{kG(R)}$, $U(R)$ is the signal at the photoreceiver from the distance R, k is the apparatus constant, $G(R)$ is the lidar geometric function; $R_{\max}$ is the maximal sounding range (the end of the sounding path). The value of $\alpha(R_{\max})$ was chosen based on the continental model by V. E. Zuev and G. M. Krekov [14]. Expression (1) is the solution of Bernoulli's standard differential equation [7, 13], which is well proven under noise conditions. In calculation, the low strobe of a ceilometer, located 19 m above the surface, was used.

The weather before the earthquake onset was stable and anticyclonal. Optically, the start of measurements was accompanied by dense haze with a ground visibility range ~3–4 km. The lidar was switched on May 11 and operated in the routine measurement mode at the instant of Sichuan earthquake onset. Since the speed of seismic waves, both longitudinal and lateral, depends mainly on the density of the terrestrial rocks and is equal to 8–10 km/s [10], it took a seismic wave a little more than a minute to reach Loyan. According to personal estimates, the transparency of the surface air layer decreased rather sharply, and then a dense haze appeared.

Figure 1 shows the lidar measurements for May 11–13, 2008. The right-hand scale presents the volume scattering coefficient $\alpha(R)$ in km^{-1}. The vertical light line shows the time of the first underground shock. Light columns in daytime denote the sky background (sunlight scattered in the atmosphere), which could not be removed completely because of the rather wide transmission band of the interferential light filter (100 nm).

It is seen in Fig. 1 that atmospheric optical parameters before and after the earthquake strongly differ. Before the start of underground shocks (to the left from the light vertical line) almost all aerosol is accumulated in the atmospheric layer from 0 to 0.5–1.0 km; several tens of minutes before the earthquake, the decrease in the surface air layer thickness and the transfer of scattering particles into higher atmospheric layers, up to 2.0–2.5 km, are observed. This fact is confirmed by Fig. 2.

There are three curves in Fig. 2 which show the altitude behavior of the scattering coefficient $\alpha(R)$ two hours before the earthquake (*1*), an hour prior to the event (*2*), and at the instant of underground shocks (*3*). The confidence intervals for curves *1–3* are calculated for a confidence probability of 0.9. The analysis of curve *1* shows that the surface air layer reaches an altitude of about 0.5 km, and the profile is smooth in general. At altitudes of 2.5 km and higher, the scattering coefficient tends to a value of 10^{-2}, which corresponds to scattering in a molecular atmosphere. The peculiar "roundness" of the profile in the lowest air layers (0–0.2 km) is explained by the inaccurate setting of the lidar geometrical function $G(R)$, which is calculated every hour in order to compensate the variability of (R) under thermal deformations of the lidar case due to solar radiation. The effect of the geometrical function in the given experiment is noticeable up to an altitude of 0.2 km.

Profile *2* (an hour prior to the earthquake onset) significantly differs from profile *1*. First of all, there is a characteristic step on the curve, which indicates the formation of the boundary layer with the top boundary at altitudes of 2.0–2.7 km.

The transfer of aerosol to the upper atmospheric layers proceeds at the cost of the ground layer reserves, which is seen from the decreasing thickness of the latter. The aerosol can be transported by atmospheric convective cells, which appear during thermal heating of the soil [11, 12] and are unrelated to the earthquake. Another cause can be the formation of microfractures on the ground surface, through which gases usually located deep under ground (hydrogen, methane, carbonic acid, etc.) enter the atmosphere. An increase in their concentration in the atmosphere serves an earthquake precursor [10]. The microfractures can be formed by stresses and shifts in the Earth's crust before earthquakes [10].

Simultaneously, an increase in the scattering coefficient above the surface air layer up to values of 2.0–2.5 km^{-1} can be noted. The state of the atmosphere at the instant of the first underground shock is shown in Fig. 2 by curve *3*: The top boundary of the boundary mixing layer has more distinct shapes up to 2.5–3.0 km, the magnitude of the scattering coefficient in the surface air layer increased up to 7–8 km^{-1} at nearly the

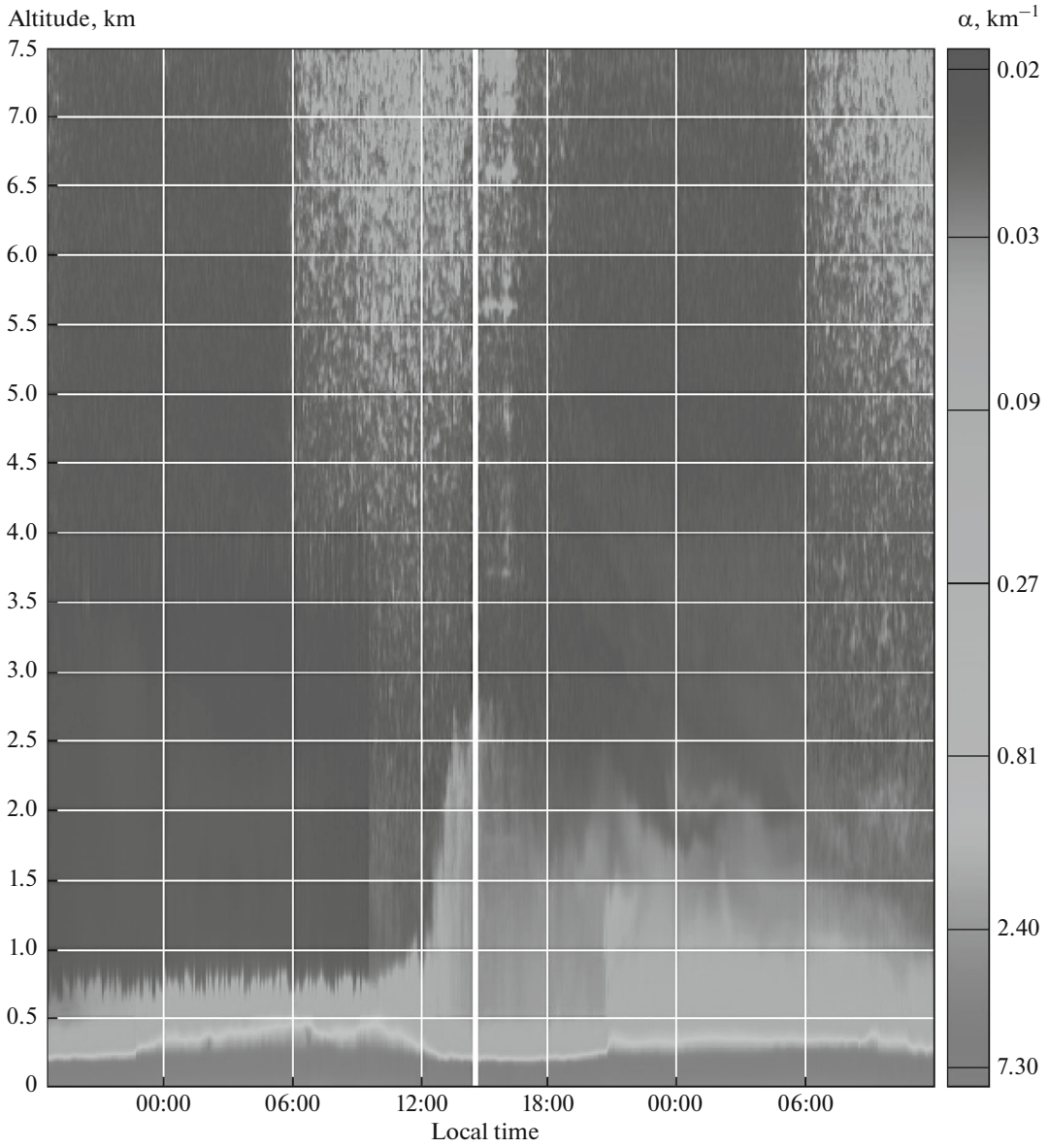

Fig. 1. Temporal behavior of the scattering coefficient profile during May, 11–13, 2008 (see color version on http://ao.iao.ru/images/ao/figures/31_01_06/01-06_colo_.jpg).

same thickness of the layer (0.25 km). Consequently, the optical depth in the surface air layer increased due to the ingress of additional aerosol mass. The scattering coefficient scarcely changed above 3 km; therefore, these layers are not shown in Fig. 2.

The earthquake continued for several minutes, and then the intensity of the underground shocks began to decrease. Figure 1 shows that the thickness of the surface layer to the right of the vertical light line (i.e., after the earthquake) gradually returned to the initial level. The recovery of the atmospheric situation took several hours.

The fact that just the earthquake was the cause of the scattering coefficient variations was confirmed by

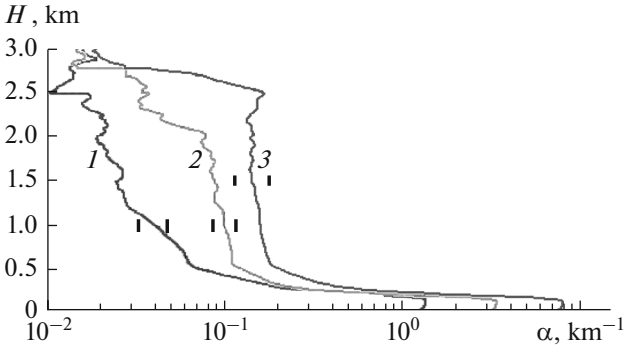

Fig. 2. Altitude profiles of the volume scattering coefficient two hours (*1*) and an hour (*2*) before the earthquake and at the instant of the event onset (*3*).

the situation of the preceding day, when the diurnal fluctuations of $\alpha(R)$ had absolutely another character under similar weather conditions.

CONCLUSIONS

—Two hours prior to the earthquake onset the atmospheric state was calm; the scattering coefficient profile was comparatively smooth, which is supported by Fig. 2.

—Approximately an hour prior to the earthquake, the profile of the scattering coefficient began to change; there appeared a characteristic step on it, which determined the top of the boundary mixing layer.

—By the instant of the first underground shock, a large amount of aerosol was observed in the atmosphere up to altitudes of 2.5–3.0 km; the scattering coefficient in the surface air layer increased up to 7–8 km^{-1}.

—A sharp variations in atmospheric optical characteristics under the conditions of stable atmosphere and in the absence of fronts can serve a predictor of an earthquake, together with a series of other geophysical signs.

—The recovery of atmospheric parameters after the earthquake termination took several hours.

REFERENCES

1. R. S. Leonard and R. A. Barnes, "Observations of ionospheric disturbance following the Alaskan earthquake," J. Geophys. Res. **70** (9), 1250–1253 (1965).
2. V. A. Liperovskii, O. A. Pokhotelov, and S. A. Shalimov, *Ionospheric Precursors of Earthquakes* (Nauka, Moscow, 1992) [in Russian].
3. E. Davies and D. M. Baker, "Ionospheric effect observed around the time of the Alaskan earthquake of March 28, 1964," J. Geophys. Res. **70** (9), 2251–2253 (1965).
4. *Short-Term Forecast of Catastrophic Earthquakes with the Use of Radio-Physics Ground- and Space-Based Methods*, Ed. by V.N. Strakhov (IPE RAS, Moscow, 1999) [in Russian].
5. V. V. Chmyrev, N. S. Isaev, and S. V. Bilichenko, "Observation by space borne detectors waves in the ionosphere over the earthquake centre," Phys. Earth Planet Inter. **57**, 110–114 (1989).
6. L. S. Ivlev, V. I. Davydova-Martines, O. A. Vargas, and A. Martines, "Variability of aerosol, ozone, and sulfur dioxide characteristics in the surface layer on earthquake in West Mexico," Atmos. Ocean. Opt. **11** (5), 428–431 (1998).
7. A. A. Tronin, "Thermal IR satellite sensor data application for earthquake research in China," Int. J. Remote Sens. **21** (6), 3169–3177 (2000).
8. G. G. Matvienko, V. A. Alekseev, A. I. Grishin, G. M. Krekov, and M. M. Krekova, "Study of fluctuations of electric and aerosol characteristics of the atmosphere as a precursor of tectonic activity," Atmos. Ocean. Opt. **8** (8), 629–637 (2007).
9. J. D. Klett, "Stable analytical inversion solution for processing lidar returns," Appl. Opt. **20** (2), 211–220 (1981).
10. C. F. Richter, *Elementary Seismology* (W.H. Freeman and Co., San Francisco, 1958).
11. A. E. Gill, *Atmosphere-Ocean Dynamics* (Academic Press, 1982).
12. A. M. Obykhov, Turbulence and Dynamics of the Atmosphere (Gidrometeoizdat, Leningrad, 1988) [in Russian].
13. G. Korn and T. Korn, *Mathematics Handbook* (Nauka, Moscow, 1977) [in Russian].
14. V. E. Zuev and G. M. Krekov, *Modern Problems of Atmospheric Optics*, Vol. 2, *Optical Models of Atmosphere* (Gidrometeoizdat, Leningrad, 1986) [in Russia].

Translated by S. Ponomareva